Enhancing associative learning in rats with a computationally designed training protocol

Xu O. Zhang; Yili Zhang; Douglas S. Engelke; Claire E. Cho; Paul Smolen; John H Byrne; Fabricio H. Do-Monte[#].

Department of Neurobiology and Anatomy, McGovern Medical School, The University of Texas Health Science Center at Houston, Houston, Texas 77030

#Corresponding author:
Fabricio H. Do Monte, DVM, PhD.
Phone: 713-500-5613
Email: fabricio.h.domonte@uth.tmc.edu

Competing Interests: The authors declare no competing interests.

Author Contributions: X.O.Z, D.S.E., and C.E.C performed and analyzed the behavioral experiments. Y.Z. implemented the computational model and ran all simulations. P.S. helped design and implement the computational model. F.H.D-M and J.H.B supervised and contributed to all aspects of this study. All the authors participated in the design of the experiments. X.O.Z. and F.H.D-M interpreted the data and prepared the manuscript with comments from all the co-authors.

Classification: Biological Sciences/Neuroscience

Keywords: Associative memory, fear conditioning, fear extinction, long-term potentiation, learning model, spaced learning.

This PDF file includes:

Main Text

Figures 1 to 5, Supplementary Figures 1 to 3

Abstract

Associative learning requires the activation of protein kinases with distinct temporal dynamics. Learning protocols with computationally designed intertrial intervals (ITIs) that maximize the interaction between fast-activated protein kinase A (PKA) and slow-activated extracellular signal-regulated kinase (ERK) enhance nonassociative learning in *Aplysia*. Here, we tested whether an optimal learning protocol with irregular ITIs, predicted computationally to increase the overlap between PKA and ERK signaling in rat hippocampus, would enhance associative learning in mammals. We simulated ~1000 training protocols with irregular ITIs and identified an optimal protocol, predicted to induce stronger associative learning than standard protocols with fixed ITIs. With auditory fear conditioning, we showed that male adult rats exposed to the optimal conditioning protocol exhibited stronger fear memory retrieval and impaired fear memory extinction, compared to rats that received either massed or spaced conditioning protocols with fixed ITIs. With fear extinction, we likewise observed that fear conditioned rats exposed to the optimal extinction protocol showed improved extinction of contextual fear memory, compared to rats that received standard extinction protocols. Together, these findings demonstrate the capacity of a behavioral intervention driven by a computational model of memory-related signaling pathways to enhance associative learning in mammals and may provide greater insight into strategies to improve cognition in humans.

Significance Statement

To test if associative learning in mammals can be enhanced by predetermined training protocols, we used a computational model of the temporal dynamics of essential biochemical cascades for learning and memory to predict an optimal training protocol in rats. Using auditory fear conditioning and fear extinction tests, we demonstrated that the optimal protocol enhanced the acquisition as well as the extinction of fear memories. Our results suggest that a non-invasive behavioral intervention guided by computational modeling can be used to enhance associative learning in mammals, with potential clinical relevance for facilitating memory formation as well as enhancing extinction-based therapies in humans.

MAIN TEXT

INTRODUCTION

Long-term memory (LTM) formation that lasts for days to years is believed to be mediated by synaptic plasticity including long-term potentiation (LTP) or its invertebrate analogue long-term facilitation (LTF), which require gene expression and protein synthesis (1-5). Studies in the last decades have investigated LTP/LTF and their underlying molecular processes as potential targets to enhance learning or restore memory deficits in laboratory animals. However, traditional interventions using systemic cognitive enhancers or intracerebral pharmacological manipulations (6-10) are either based on trial-and-error approaches in specific model systems or are highly invasive, making the translation of such interventions difficult for human applications. The recent

72 development of neural recording and optogenetic techniques has enabled precise
73 control of neurons based on their intrinsic firing rates in order to enhance learning or
74 modify memories (11-14), but the use of these techniques in humans remains
75 unforeseeable in the near future.
76
77 An alternative approach to enhance learning and memory is to develop computational
78 models to predict optimal training protocols based on the intracellular molecular
79 cascades that underlie LTM formation and LTP/LTF induction (15-17). Previous studies
80 have identified activation of PKA (18-20) and of the mitogen-activated protein kinase
81 (MAPK) isoform ERK (21-23) as essential cascades for LTF. These two pathways
82 converge to phosphorylate transcriptional factors such as cAMP responsive element
83 binding protein (CREB), which subsequently induce expression of multiple plasticity-
84 related genes (24-26). The observation that that these two pathways exhibit distinct
85 kinetics of activation (17, 20, 27), suggests that the temporal activity patterns, and
86 activation overlap, of these pathways may constitute an important target to enhance
87 associative learning. Accordingly, our previous study demonstrated that a
88 computationally designed protocol with irregular ITIs predicted to maximize the overlap
89 of PKA and ERK activities enhances LTF and nonassociative learning, specifically the
90 long-term sensitization of the tail elicited siphon-withdrawal reflex in *Aplysia* (28).
91
92 Substantial similarities between molecular processes of LTF in invertebrates and LTP in
93 mammals make it plausible that the same strategies used to enhance LTF and
94 nonassociative learning in invertebrates could enhance LTP and associative learning in

95 mammals. PKA activation in rodent hippocampus and amygdala is required for LTP and
96 LTM (29, 30). Similarly, activation of ERK/MAPK cascades and their cross-talk with PKA
97 kinase are required for the phosphorylation of CREB and LTP induction (31, 32). Albeit
98 with different kinetics than observed in invertebrates, PKA and ERK activation in
99 mammals also differ considerably in temporal dynamics (33-35), providing a similar
100 opportunity to maximize their overlap with irregular ITIs in an attempt to enhance
101 memory formation.
102
103 Here, we tested if the invertebrate LTF model (28) can be adapted to computationally
104 design an optimal associative learning protocol in mammals. Empirical data from the
105 literature were used to model PKA and ERK dynamics in rat hippocampus (33-35), a
106 critical brain region implicated in the formation of associative memories in mammals
107 (36-38). Then we simulated ~1000 different training protocols with irregular ITIs and
108 identified an optimal protocol, predicted to induce stronger memory than standard
109 training protocols with fixed ITIs. Using auditory fear conditioning and fear extinction
110 paradigms in rats, we confirmed that our computationally designed protocol enhanced
111 the acquisition as well as the extinction of fear memories in mammals. This strategy
112 may have potential clinical relevance for interventions aiming at facilitating memory
113 formation in psychiatric disorders associated with cognitive impairment in humans, as
114 well as to enhance extinction-based therapies in patients suffering from fear-related
115 disorders.
116
117

118 **RESULTS**

119 ***A computational model based on PKA and ERK dynamics in rats identified an***

120 ***optimal partial fear conditioning protocol***

121

122 Our model previously used in *Aplysia* (28) was adapted to simulate the dynamics of

123 PKA and ERK during the process of LTP induction in rat hippocampus (**Fig. 1A**). In this

124 model, the stimulus (*Stim*), which represents tetanic stimuli, rapidly activates PKA via

125 the cAMP pathway and slowly activates ERK via the Raf-MEK pathway. The synergistic

126 interaction between PKA and ERK pathways is quantified by a variable *inducer*, which

127 corresponds to the efficacy of the stimulus in inducing LTP. ERK kinetics were

128 described by differential equations (see Methods) with parameter values reproducing

129 empirical findings that ERK activity reaches peak levels 15~20 min after BDNF

130 treatment or tetanic stimuli in rat hippocampus acute slices (35, 39). Equations

131 describing PKA kinetics simulated data showing that PKA is transiently activated within

132 2 min after LTP induction in slices from rat hippocampus or within 5 min *in vivo* after

133 spatial discrimination task training (33, 34). We used this model to simulation fear

134 conditioning in rats, in which the pairing of a conditioned stimulus (CS) with an

135 unconditioned stimulus (US) is represented by *Stim*, and the conditioned responses are

136 proportional to the peak value of *inducer*. We observed that a single CS-US pairing

137 produced little overlap between PKA and ERK pathways (**Fig. 1B1**). We then simulated

138 ~1000 partial fear conditioning protocols, with 4 trials and varying ITIs, to identify one

139 predicted to have optimal ITIs for triggering downstream gene activation. To compare,

140 we also simulated a Full Conditioning (FC) protocol with 8 trials and a fixed ITI of 270 s,

141 and a Partial Conditioning (PC) protocol with 4 trials and the same ITI of 270 s, which
142 resemble previous protocols used for full and partial fear conditioning in rats (40, 41).
143 Our simulation identified an Optimal Partial Conditioning (OPC) protocol with 4 trials and
144 irregular ITIs of 8, 8, and 16 min, which was able to produce higher peak *inducer* than
145 the standard PC protocol (**Fig. 1B2-1B4**). Comparing OPC and PC in Fig. 1B3-B4, both
146 protocols produced pERK curves with similar peak levels (orange). However, PKA
147 activity induced by the last trial of OPC had a much larger overlap with the pERK curve
148 than did PKA induced by PC. Therefore, OPC induced a much higher peak level of
149 *inducer* (purple). Based on our simulation, we predicted that the computationally
150 designed OPC protocol would produce stronger long-term memory in rats than the
151 standard PC protocol.
152
153 ***The optimal partial conditioning protocol induces stronger fear memory than a***
154 ***standard partial conditioning protocol***
155
156 To test if the computationally designed OPC protocol could enhance associative
157 learning in rats, we used a classical auditory fear conditioning paradigm. Because the
158 hippocampus is required for context encoding during fear conditioning (42-44), we used
159 two different chambers (context A and context B) to assess the contribution of the
160 context to the auditory fear memory. The two contexts differed in size, floor texture,
161 visual decoration of the walls, and odor cues (**Fig. 2A**). On Day 0, rats were pre-
162 exposed to context A for 20 min to familiarize with the chamber where fear conditioning
163 took place in the following day. After matching their baseline freezing and locomotor

activity during the familiarization session (**Fig. S1**), rats were assigned to one of the three experimental groups described above in our simulation experiments: Full Conditioning (FC), Partial Conditioning (PC), and Optimal Partial Conditioning (OPC). On Day 1, rats were placed into context A and exposed to one nonreinforced habituation tone (3 kHZ, 75 dB, 30 s) followed by distinct fear conditioning protocols (44 min duration, **Fig. 2B**). The FC group received eight presentations of CS (3 kHZ tone, 75 dB, 30 s) that co-terminated with an US (footshock, 0.7 mA, 0.5 s) with ITIs of 270 s. The PC group received four similar CS-US pairings with the same ITIs of 270 s, and remained in the chamber until the end of the session to equate the total context exposure time. The OPC group received four similar CS-US pairings with ITIs of 8, 8, and 16 min. All groups reached high levels of freezing (> 65%, **Fig. 2C**) and reduced locomotion at the end of the fear acquisition session. On Day 2, rats were placed in context B and given two CS presentations (ITI of 150 s, 7 min duration) in the absence of US to test the retrieval of tone-associated fear memory in a novel context. Compared to the FC group, both PC and OPC groups exhibited less freezing during the second CS presentation (Two-way repeated measures (RM) ANOVA followed by Tukey's post-hoc test. $F_{(2, 37)} = 3.751$, $P = 0.033$; FC vs. OPC: p = 0.029; FC vs. PC: p = 0.002; OPC vs. PC: p = 0.527). Nevertheless, both FC and OPC groups showed reduced average speed during the retrieval test compared to the standard PC group, suggesting stronger fear retrieval in a novel context (**Fig. 2D;** One-way ANOVA followed by Tukey's post hoc test. $F_{(2, 37)} = 10.87$, $P < 0.001$; FC vs. OPC: p = 0.131; FC vs. PC: p < 0.001; OPC vs. PC: p = 0.024). On Day 3, rats were returned to context A for an extinction training session where they received twelve CS presentations (ITIs of 150 s, 37 min duration).

Although no significant differences in freezing levels were observed among the groups during each CS presentation (Two-way RM ANOVA. $F_{(22, 407)} = 1.169$, $P = 0.271$), a within session extinction analysis comparing the first four CSs to the last four CSs revealed impaired extinction learning in the FC and OPC groups, when compared to the PC group. This impairment in the acquisition of extinction in the FC and OPC groups was characterized by sustained freezing levels across the session, which differed from the PC group that showed reduced freezing levels from the first to the last CSs presentation (**Fig. 2E left;** Paired Student's t test. FC: $t_{13} = 2.153$, p = 0.051; PC: $t_{11} = 4.191$, p = 0.001; OPC: $t_{13} = 0.869$, p = 0.400**)**. Interestingly, the OPC group exhibited persistent freezing levels during the extinction training session as indicated by a reduced relative change in freezing from the beginning to the end of the session, when compared to the PC group (**Fig. 2E right;** One-way ANOVA followed by Tukey's post-hoc test. $F_{(2, 37)} = 3.315$, $P = 0.047$; FC vs. OPC: p = 0.487; FC vs. PC: p = 0.320; OPC vs. PC: p = 0.037). Despite the persistent freezing levels across the extinction training session observed in the OPC group, no significant differences were found between the OPC and the PC groups during either the extinction retrieval tests performed on Days 4 and 5 (Two-way RM ANOVA. context A: $F_{(2, 37)} = 0.097$, $P = 0.907$; context B: $F_{(2, 37)} = 2.984$, $P = 0.063$) or the spontaneous recovery tests performed on Days 29 and 30 (**Fig. 2C;** Two-way RM ANOVA followed by Tukey's post hoc test. context A: $F_{(2, 37)} = 3.259$, $P = 0.049$; FC vs. OPC: p = 0.027; FC vs. PC: p = 0.038; OPC vs. PC: p = 0.999; context B: $F_{(2, 37)} = 0.774$, $P = 0.469$). Taken together, these data demonstrate that the computationally designed training protocol (OPC) is able to enhance fear acquisition in rats, thereby resulting in a stronger fear memory that is more resistant to extinction.

210

211 ***The optimal partial conditioning protocol induces stronger fear memory than a***

212 ***spaced partial conditioning protocol***

213

214 Previous studies have demonstrated that spaced learning protocols result in stronger

215 memories than standard (i.e., massed) learning protocols in both humans (45, 46) and

216 rodents (47-49, but also see 50). Thus, an alternative explanation for the augmented

217 fear memory observed in the OPC group in Fig. 2 could be simply a trial-spacing effect,

218 because our standard PC group used massed CS-US pairings. Both protocols produced

219 similar peak values of the pERK curves, but different overlap of PKA and ERK activities,

220 suggesting a way in which appropriately spaced protocols might advantageously

221 enhance overlap of kinase activities with distinct dynamics. Indeed, there was a broad

222 range of effective 4-trial protocols (**Fig. S2**), with one protocol with fixed 11 min 10 s ITIs

223 producing a nearly identical peak level of inducer as the OPC protocol, and a higher

224 peak level of inducer than other protocols with fixed ITIs from 1 min to 21 min (**Fig. 3A1,**

225 **Fig. S2A**). We termed this protocol the spaced partial conditioning (SPC) protocol. We

226 also examined the effects of different stimulus intensities on predicting optimal training

227 trials. The 1,000 different protocols were re-simulated with a reduced intensity of

228 stimulus. Interestingly, the protocol with 4 trials and irregular ITIs of 8, 8, and 16 min

229 still produced the greatest peak level of inducer (**Fig. 3A2, Fig. S2B**). Equally

230 interesting was that with weaker stimuli, the OPC protocol became relatively more

231 effective than the SPC protocol. Therefore, we predicted that empirically, the irregular

232 intervals of the OPC may produce more effective conditioning than the SPC protocol. To

233 test this hypothesis, we conducted an experiment to compare the OPC and SPC
234 protocols using a reduced shock intensity (0.5 mA instead of the 0.7 mA used in Fig. 2)
235 (**Fig. 3B**). Rats were assigned to OPC or SPC groups by matching their baseline
236 freezing and locomotor activity during the familiarization session (**Supplementary Fig.**
237 **1B**). During the fear acquisition, the SPC group received 4 CS-US pairings with ITIs of
238 11 min and 10 s, whereas the OPC group was exposed to the same protocol as in Fig.
239 2 (*i.e.*, 4 CS-US pairings with ITIs of 8, 8, and 16 min) (**Fig. 3C**). We found that the
240 difference in the ITIs between the OPC and SPC groups was sufficient to result in
241 distinct levels of fear memory acquisition. Rats exposed to OPC showed higher CS
242 freezing levels during the third CS-US pairing of the fear acquisition session (**Fig. 3D**
243 **Day 1;** Two-way RM ANOVA followed by Tukey's planned comparison. $F_{(4, 64)} = 1.550$,
244 $P = 0.339$; OPC vs. SPC: p = 0.019). In addition, fear memory retrieval was increased
245 when rats in the OPC group were returned to context A for an extinction training session
246 on Day 3, as indicated by higher freezing during the first two CS presentations,
247 compared to the SPC group (**Fig. 3D Inset;** Welch's t test. $t_{12.43} = 2.227$, p = 0.045).
248 Both OPC and SPC groups exhibited the same levels of freezing by the end of the
249 extinction training session (**Fig. 3D Day 3;** Two-way RM ANOVA followed by Tukey's
250 post hoc test. $F_{(11, 176)} = 2.997$, $P = 0.001$; Tone 12, OPC vs. SPC: p > 0.999), as well as
251 during the extinction retrieval tests performed in context A (**Fig. 3D Day 4;** Two-way RM
252 ANOVA. $F_{(2, 37)} = 0.097$, $P = 0.907$) or context B (**Fig. 3D Day 5;** Two-way RM ANOVA.
253 $F_{(2, 37)} = 2.984$, $P = 0.629$). However, fear memory spontaneously recovered when rats
254 in the OPC group were retested in context A approximately 3 weeks later, as indicated
255 by higher freezing during the first CS presentation compared to SPC-trained rats (**Fig.**

256 **3D Day 29;** Two-way RM ANOVA followed by Tukey's planned comparison. $F_{(2, 32)}$ =
257 1.809, P = 0.180; OPC vs. SPC: p = 0.030). In summary, these data suggest that the
258 enhancement in fear memory acquisition observed with our computationally designed
259 OPC protocol cannot simply be attributed to a trial-spacing effect or differences in the
260 delay to remove the animals from the chamber, but it is rather associated with the
261 maximized overlap between PKA and ERK signaling.
262
263 ***The computationally designed optimal partial conditioning protocol also***
264 ***enhanced fear extinction***
265
266 Extinction is a new learning that temporarily inhibits the initial associative memory (51,
267 52). Because previous studies suggest that the molecular mechanisms underlying fear
268 extinction learning are similar to those underlying fear acquisition (53-58), we
269 hypothesized that the computationally designed protocol would also enhance the
270 acquisition of extinction, suppressing the original fear memory. We therefore used the
271 OPC protocol with 4 trials and irregular ITIs of 8, 8, and 16 min as an Optimal Partial
272 Extinction (OPE) protocol (**Fig. 4B4**). We compared the OPE protocol with a Full
273 Extinction (FE, **Fig. 4B2**) protocol using 12 trials and ITIs of 150 s, and a Partial
274 Extinction (PE, **Fig. 4B3**) protocol using 4 trials and the same ITIs of 150 s, which
275 resemble previous protocols used for full and partial fear extinction in rats (59-61).
276 Similar to the simulation results for the conditioning protocols, the OPE protocol
277 triggered higher peak *inducer* than the PE protocol with equal ITIs of 150 s, and was

comparable to the FE protocol (**Fig. 4B**). We thus predicted the OPE protocol would result in stronger extinction of fear memory than the standard PE protocol.

To test this prediction, we designed an experiment comparing the efficacy of different extinction protocols (**Fig. 5A**). We used conditioned suppression of reward-seeking behavior as an additional measure of fear memory because lever-press suppression is more sensitive than freezing during fear extinction paradigms (62, 63). In addition, lever presses help to maintain a constant level of activity so that freezing can be more reliably measured along the session (64). Since lever presses for reward are trained in a specific context, and extinction memory is context-dependent (65, 66), we used only one context in this experiment so that lever press suppression can be consistently assessed across sessions and the extinction memory can be retrieved after the extinction learning. Rats were initially trained to press a lever to receive sucrose pellets in a variable interval schedule of 60 s. After 7 days of training, rats reached the same levels of lever pressing (~10 presses/min) and locomotor activity (**Supplementary Fig. 1C**). On Day 8, they underwent a fear conditioning session which included five nonreinforced habituation tones (3 kHZ, 75 dB, 30 s duration) followed by seven CS-US pairings (ITIs of 150 s, 37 min duration). In simulations, the OPE group showed peak levels of *inducer* comparable to the FE group and higher than the PE group when strong stimuli were used. We therefore increased the footshock intensity from 0.7 mA to 1.0 mA, which resulted in stronger fear acquisition and consequently higher freezing levels during the extinction session. This stimulus intensity also helped to avoid a “floor effect” in the following tests. On Day 9, rats were assigned to three experimental groups by

301 matching their freezing and lever presses during the fear conditioning session: Full
302 Extinction (FE), Partial Extinction (PE), and Optimal Partial Extinction (OPE) (One-way
303 ANOVA. $F_{(14, 231)} = 0.404$, $P = 0.973$). On Day 10, rats were returned to the same
304 chamber for a fear extinction session (39 min duration). The FE group received twelve
305 CSs with ITIs of 150 s; the PE group received four CSs with ITIs of 150 s and remained
306 in the chamber until the end of the session; and the OPE group received four CSs with
307 ITIs of 8, 8, and 16 min (**Fig. 5B**). Our results revealed that at the end of the CS
308 presentations, freezing levels reduced from ~50% to ~20% in the FE groups, whereas
309 the PE and OPE groups maintained the same levels of freezing throughout the four CSs
310 (**Fig. 5C, Day 8**). Similarly, the FE group showed a significant increase in lever presses
311 (from 0.1 to 1.5 press/min) during the CS presentations from the beginning to the end of
312 the session, whereas CS lever presses remained unaltered in the PE and OPE groups
313 (**Supplementary Fig. 3A&B**; Paired Student's t test; FE: $t_{11} = 2.837$, p = 0.016; PE: t_{10}
314 = 1.000, p = 0.341; OPE: $t_{12} = 1.237$, p = 0.239). However, the OPE group showed a
315 significant increase in lever presses during the 30-s periods that preceded the CS
316 presentations (pre-CS) when comparing the first two pre-CS periods to the last pre-CS
317 period of the extinction training session (**Fig. 5D&E**; Paired Student's t test; FE: t_{11} =
318 0.994, p = 0.341; PE: $t_{10} = 1.111$, p = 0.293; OPE: $t_{12} = 3.773$, p = 0.003), suggesting
319 enhanced within-session extinction of contextual fear memory (67). On Days 10 and 35,
320 rats were returned to the same chamber and received two CSs with an ITI of 150 s to
321 test the strength of fear extinction memory during extinction retrieval and spontaneous
322 recovery tests, respectively. No significant difference in CS freezing or CS lever presses
323 were observed among the three groups during these tests (**Fig. 5C, Day 10&35;** Two-

324 way RM ANOVA. Day 10: Freezing, $F_{(2, 33)} = 0.207$, $P = 0.814$; Lever Presses, $F_{(2, 33)} =$
325 0.069, $P = 0.933$; Day 35: Freezing, $F_{(2, 33)} = 0.535$, $P = 0.591$; Lever Presses, $F_{(2, 33)} =$
326 1.085, $P = 0.350$). However, the OPE group showed increased pre-CS lever pressing
327 rate either in the first pre-CS period (**Fig. 5D;** Two-way RM ANOVA followed by Tukey's
328 planned comparison. $F_{(2, 33)} = 2.897$, $P = 0.069$; Tone 1, a, FE vs. PE, p = 0.791; b, FE
329 vs. OPE, p = 0.025; c, OPE vs. PE, p = 0.005) or when averaging the two pre-CS
330 periods during the spontaneous recovery test (**Fig. 5F**; Kruskal-Wallis's test followed by
331 Dunn's post hoc test. $H(2) = 6.414$, $P = 0.041$; a: FE vs. OPE, p = 0.531; b: FE vs. PE, p
332 = 0.709; c: OPE vs. PE, p = 0.035), when compared to the FE and PE groups on day
333 35. These results suggest that, although the tone-associated memory was similar
334 among the groups, our computationally designed OPE protocol was able to enhance the
335 extinction of contextual fear memory, as indicated by enhanced within-session
336 extinction of conditioned suppression and by reduced conditioned suppression
337 approximately 3 weeks after the extinction training session.
338
339 **DISCUSSION**
340
341 Studies on nonassociative learning in invertebrates have provided significant insights
342 about the molecular mechanisms of learning and memory due to their simplicity and
343 tractability (2, 5, 68). Long-term nonassociative learning in different regions of the
344 nervous system or across different species shares many intracellular molecular
345 cascades including cAMP-PKA and Raf-MEK-ERK signaling (21, 25). These two
346 pathways are also required for associative learning in invertebrates and mammals (29,

347 31, 69). The conservation of these mechanisms makes these molecular cascades
348 potential candidates for a universal intervention to enhance learning and memory. We
349 have previously demonstrated that a computationally designed protocol that maximizes
350 the interaction between PKA and ERK pathways enhances LTF and nonassociative
351 learning in *Aplysia* (28). Here, we extended the feasibility of this computational
352 approach to associative learning in mammals by adapting the simplified mathematical
353 model used in *Aplysia* to simulate the dynamics of PKA and ERK in rat hippocampus
354 based on empirical data available in the literature (33-35). After simulating ~1000
355 different training protocols of auditory fear conditioning, we identified an optimal protocol
356 with irregular ITIs which resulted in stronger fear acquisition and extinction-resistant
357 memory formation in rats, when compared to either massed or spaced training protocols
358 with equal ITIs. Using a separate fear extinction paradigm, we also showed that an
359 optimal training protocol was sufficient to induce enhanced extinction of contextual fear
360 memory in rats, when compared to standard or partial extinction protocols with equal
361 ITIs. Our results demonstrate the power of a simplified model of intracellular signaling
362 cascades in guiding associative learning across species, attesting the essential role of
363 the interaction between PKA and ERK pathways in both nonassociative and associative
364 learning. In addition, our findings highlight the potential clinical relevance of using
365 computational modeling to enhance associative learning in patients with memory
366 deficits, as well as to enhance extinction-based exposure therapies in patients with
367 anxiety disorders.
368

369 Pioneering studies have demonstrated that training protocols using spaced ITIs result in
370 stronger memory acquisition than those using standard massed ITIs, a well-established
371 phenomenon described as the “trial-spacing effect” (see review by 15). Data
372 demonstrating this effect in animals and humans illustrate the relationship between the
373 duration of the ITIs and the strength of memory formation as an inverted-U-shape curve
374 (70, 71), consistent with our simulated results (Fig. 1C). Previous findings have
375 attributed this spacing effect to the different efficacy of massed vs. spaced protocols in
376 inducing LTP/LTF through plasticity-related signaling. For instance, spaced training
377 protocols in rodents lead to increased activation of ERK (72), followed by CREB
378 phosphorylation and the expression of downstream genes, which have not been
379 reported following massed training protocols in the same species (73). A computational
380 model based on slice electrophysiology from rat hippocampal data has found that the
381 peak of ERK activation aligns with the optimal ITI for LTP induction (39). Although that
382 study provided a possible mechanism for the trial-spacing effect and a potential
383 approach to identify more effective protocols for associative learning, it relied on fixed
384 ITIs that are not necessarily the optimal intervals to induce synaptic plasticity and LTM.
385 In fact, our simulations showed that an optimal protocol with irregular ITIs was superior
386 to most spaced protocols with the same number of trials and equal ITIs. In the fear
387 conditioning experiment, the optimal protocol induced stronger and persistent fear
388 memory in rats, when compared to a spaced protocol predicted to be the most efficient
389 among protocols with equal ITIs. These results suggest that the trial-spacing effect in
390 mammals can be at least partially explained by enhanced overlap between PKA and
391 ERK pathways, which are critical for CREB activation (32). More importantly, our

392 findings demonstrate that protocols that include irregular ITIs can be a better approach
393 to enhance learning than previous protocols using equal ITIs.
394
395 The enhanced performance of our optimal protocol (OPC) compared to a spaced
396 protocol (SPC) during fear conditioning appears constrained by the intensity of stimuli.
397 The model predicts higher performance for OPC when weak stimuli are used, but
398 comparable performance when strong stimuli are used (**Fig. 3A**). Drawing a line to
399 distinguish weak and strong footshock intensities is not straightforward because the
400 relationship between fear memory and footshock intensity is neither monotonic nor
401 linear (74). Nevertheless, we observed clear differences in the efficacy of the optimal
402 fear conditioning protocol when using footshocks of different intensities. When we
403 compared the optimal partial conditioning protocol to a massed partial conditioning
404 protocol using a standard footshock intensity (0.7 mA, **Fig.2**) commonly used in
405 previous studies (30), we found only small differences in the conditioned responses (CS
406 freezing) between the two protocols. However, when we used a lower footshock
407 intensity (0.5 mA, **Fig.3**) to compare the optimal partial conditioning protocol to a
408 spaced partial conditioning protocol, we found a significant increase in CS freezing in
409 the OPC group during fear acquisition, retrieval, and spontaneous recovery tests.
410 Considering the robustness of the trial-spacing effect, it is possible that differences
411 between the OPC and the massed PC groups at the higher footshock intensity were
412 masked by a “ceiling effect”. These data suggest that our approach could be more
413 beneficial for learning protocols relying on relatively weak stimuli. Additional studies
414 need to be conducted to understand the mechanism by which the intensity of stimuli

415 determines the enhanced performance of protocols with irregular ITIs compared to
416 protocols with fixed ITIs.
417
418 The association between the CS and US is primarily mediated by the lateral amygdala
419 where LTP induces enhanced CS responses (see review by 75, 76). Nevertheless,
420 another important and distinguishable component of fear memory formation is the
421 context in which the association has occurred. In the fear conditioning experiment,
422 enhanced CS freezing by our computationally designed protocol was only observed in
423 the same context where fear conditioning took place, suggesting that the memory
424 facilitation effect induced by our optimal protocol is context dependent. Similarly, in the
425 fear extinction experiment, enhancement by the optimal protocol was only observed
426 during the pre-CS lever pressing, a more sensitive index of contextual fear memory
427 during extinction and spontaneous recovery (62, 63, 67, 77, 78). These results are
428 consistent with the fact that the model is based on empirical data from rat hippocampus
429 currently available in the literature. The hippocampus plays major roles in context
430 encoding during fear conditioning, fear extinction, and the time-dependent
431 reappearance of fear following extinction training (*i.e.*, spontaneous recovery) (see
432 reviews by 44, 79). The observation that the temporal dynamics of ERK pathways differ
433 across brain regions involved in fear memory, with peaks occurring at 20 min after
434 stimulation in the hippocampus versus 60 min after fear conditioning in the lateral
435 amygdala (35, 80, 81) , suggests that the model may be able to predict optimal
436 protocols targeting specific components of fear memory based on the dynamics of
437 intracellular signaling cascades in distinct brain regions. Future studies will test this

438 possibility by modeling the molecular cascades in the lateral amygdala to preferentially
439 target the acquisition and extinction of CS-associated memories.
440
441 It is worth noting that the model is an extremely simplified one. We did not consider
442 many other important molecular cascades critical for LTP and memory formation. For
443 example, calcium/calmodulin-dependent protein kinase II (CaMKII) and protein kinase C
444 (PKC) are also required for LTP induction (16, 82, 83). In addition, we built the model
445 with empirical data of PKA and ERK dynamics from the literature, which are based on
446 *ex vivo* analyses and have limited temporal resolution. However, despite these
447 limitations, we demonstrated that the simplified model using essential biochemical
448 cascades for learning and memory was sufficient to enhance associative learning in
449 three different experiments in mammals. A more complex model that incorporates a
450 wider range of intracellular and extracellular processes based on *in vivo* real-time data
451 may strengthen the predictive ability of simulations. Further experiments should also
452 investigate whether the memory enhancing effects of our optimal protocol vary across
453 subjects of different sexes and ages, as well as its efficacy in animal models of cognitive
454 impairment. Together, our results suggest the possibility of using similar model-driven,
455 non-invasive behavioral approaches in preclinical and clinical studies aimed at
456 enhancing learning or restoring memory deficits in humans.
457
458
459 **MATERIALS AND METHODS**
460 **Animals**

461 All experimental procedures were approved by the Center for Laboratory Animal
462 Medicine and Care of The University of Texas Health Science Center at Houston.
463 National Institutes of Health guidelines for the care and use of laboratory animals were
464 strictly followed in order to minimize any potential discomfort and suffering. A total of
465 120 male Long-Evans hooded adult rats (Charles Rivers Laboratories) 3-5 months of
466 age and weighing 330-450 g were used. Rats were kept in a 12-hour light/12-hour dark
467 cycle with food and water *ad libitum*. Experiments were conducted during the light
468 phase. For the Optimal Extinction experiment, animals were maintained on a restricted
469 diet of 18 g per day of standard laboratory rat chow to increase their motivation during
470 the lever press training. Rats' weights were monitored weekly to make sure that all
471 animals maintained their weight under food restriction.
472
473 **Model Development**
474 The mathematical model for the activation of kinase cascades critical for long-term
475 memory (LTM) was modified from a previous model of the signaling cascades for the
476 induction of long-term synaptic facilitation (28). As mentioned above, the induction of LTM
477 for fear conditioning is known for requiring the activation of multiple kinase cascades with
478 different temporal dynamics. In the model, the cyclic AMP (cAMP)-PKA pathway is rapidly
479 activated after training, whereas the Raf- MEK-ERK pathway is slowly activated, and both
480 are required for the induction of LTM after fear conditioning and extinction (**Fig. 1A, Fig.**
481 **4A**).
482 PKA Pathway. The dynamics of cAMP activation upstream of PKA following
483 training and the cAMP-dependent activation of PKA are described by Eqs. 1-4. Inactive

484 PKA is a holoenzyme (PKA_{RC}, Eq. 2), consisting of regulatory (PKA_R, Eq. 3) and catalytic
485 (PKA_C, Eq. 4) subunits. In response to training, represented by the variable *Stim* in Eq.
486 1, cAMP is activated (Eq. 1). Active cAMP binds to the regulatory subunit of PKA, leading
487 to the release of free, active catalytic subunit (Fig. 1A) (Eqs. 2-4). '*Stim*' represents the
488 neurotransmitters released by training that function to activate kinase cascades.
489

490 $$\frac{d[cAMP]}{dt} = \lambda \frac{[Stim]}{[Stim] + K_{Stim}} - k_{b,cAMP}[cAMP] \qquad \text{(Eq. 1)}$$

491 $$\frac{d[PKA_{RC}]}{dt} = k_{b,PKA}[PKA_C][PKA_R] - k_{f,PKA}[PKA_{RC}][cAMP]^2 \qquad \text{(Eq. 2)}$$

492 $$\frac{d[PKA_R]}{dt} = k_{f,PKA}[PKA_{RC}][cAMP]^2 - k_{b,PKA}[PKA_C][PKA_R] \qquad \text{(Eq. 3)}$$

493 $$\frac{d[PKA_C]}{dt} = k_{f,PKA}[PKA_{RC}][cAMP]^2 - k_{b,PKA}[PKA_C][PKA_R] \qquad \text{(Eq. 4)}$$

494 Parameter values are modified from (28) to activate PKA immediately after training, but
495 with PKA activity quickly returning to the basal in ~5 min (Fig. 1B) (33, 34): λ = 14.6
496 μM/min, K_{STIM} = 85 μM, $k_{b,cAMP}$ = 4 min^{-1}, $k_{f,PKA}$ = 20 $\mu M^{-2}min^{-1}$, $k_{b,PKA}$ = 12
497 $\mu M^{-1}min^{-1}$
498

499 <u>ERK Pathway.</u> The activation of ERK by training '*Stim*' is via sequential activation
500 of the upstream kinases Raf and MEK (Fig. 1A). Raf activates the MAP kinase kinase
501 MEK, MEK in turn activates the MAP kinase ERK. The differential equations describing
502 the activation of Raf, MEK, and ERK (Eqs. 5-12) are similar to those in (28). However, a
503 discrete time delay in activation of Raf was removed from the phosphorylation of Raf (Eq.
504 5). Instead, based on empirical data (35, 39), parameters describing the activation of Raf

505 were adjusted from (28) so that the ERK activation curve reached the peak around 20

506 min post-training (Fig. 1B).

507 $$\frac{d[Raf^p]}{dt} = k_{f,Raf}[Raf][Stim] - k_{b,Raf}[Raf^p] \quad \text{(Eq. 5)}$$

508 $$[Raf] = [Raf]_{total} - [Raf^p] \quad \text{(Eq. 6)}$$

509 $$\frac{d[MEK]}{dt} = \frac{k_{b,MEK}[MEK^p]}{[MEK^p] + K_{MEK,2}} - \frac{k_{f,MEK}[Raf^p][MEK]}{[MEK] + K_{MEK,1}} \quad \text{(Eq. 7)}$$

510 $$\frac{d[MEK^{pp}]}{dt} = \frac{k_{f,MEK}[Raf^p][MEK^p]}{[MEK^p] + K_{MEK,1}} - \frac{k_{b,MEK}[MEK^{pp}]}{[MEK^{pp}] + K_{MEK,2}} \quad \text{(Eq. 8)}$$

511 $$[MEK^p] = [MEK]_{total} - [MEK] - [MEK^{pp}] \quad \text{(Eq. 9)}$$

512 $$\frac{d[ERK]}{dt} = \frac{k_{b,ERK}[ERK^p]}{[ERK^p] + K_{ERK,2}} - \frac{k_{f,ERK}[MEK^{pp}][ERK]}{[ERK] + K_{ERK,1}} \quad \text{(Eq. 10)}$$

513 $$\frac{d[ERK^{pp}]}{dt} = \frac{k_{f,ERK}[MEK^{pp}][ERK^p]}{[ERK^p] + K_{ERK,1}} - \frac{k_{b,ERK}[ERK^{pp}]}{[ERK^{pp}] + K_{ERK,2}} \quad \text{(Eq. 11)}$$

514 $$[ERK^p] = [ERK]_{total} - [ERK] - [ERK^{pp}] \quad \text{(Eq. 12)}$$

515 Parameter values: $k_{f,Raf}$ = 0.001 $\mu M^{-1} min^{-1}$, $k_{b,Raf}$ = 0.05 min^{-1}, $[Raf]_{total}$ = 0.5 μM,

516 $k_{f,MEK}$ = 0.41 min^{-1}, $k_{b,MEK}$ = 0.04 μM/min, $K_{MEK,1}$ = 0.20 μM,

517 $K_{MEK,2}$ = 0.19 μM, $[MEK]_{total}$ = 0.5 μM, $k_{f,ERK}$ = 0.41 min^{-1},

518 $k_{b,ERK}$ = 0.12 μM/min, $K_{ERK,1}$ = 0.19 μM,

519 $K_{ERK,2}$ = 0.21 μM, $[ERK]_{total}$ = 0.5 μM.

520 As in (28), a variable '*inducer*' was used to quantify the overlap of activation
521 between PKA and ERK, which together regulate the gene expression necessary for the
522 induction of LTM.

523 $$inducer = k_{inducer}\,[PKA_C]\,[ERK^{pp}] \qquad \text{(Eq. 13)}$$

524 where $k_{inducer}$ = 1 μM^{-1}.

525 To determine which protocols could more effectively activate *inducer,* four-trial
526 protocols with three ITIs, each ranging from 2–20 min in steps of 2 min, were simulated.
527 Combining these permutations yielded 10^3 protocols. For each protocol, the maximal
528 (peak) overlap between PKA and ERK was quantified as the peak level of *inducer*
529 produced. Also, the value of *Stim* was varied from 100 to 300 μM to represent weak and
530 strong trainings and to test the robustness of protocols. Based on the maximal overlap,
531 a protocol with ITIs of 8, 8, and 16 min was selected and was denoted optimal partial
532 conditioning (OPC). We assumed that fear conditioning and extinction activate the same
533 signaling pathways, so we predicted this protocol would similarly enhance extinction.

534 Numerical methods. Fourth-order Runge-Kutta integration was used for
535 integration of all differential equations with a time step of 3 s. Further time step reduction
536 did not lead to significant improvement in accuracy. The steady-state levels of variables
537 were determined after at least one simulated day, prior to any manipulations. The model
538 was programmed in XPPAUT (http://www.math.pitt.edu/~bard/xpp/xpp.html) (84) and
539 simulated on Dell Precision T1700 microcomputers.

540

541 **Behavioral Tasks**

542 ***Optimal Conditioning***

543 *Apparatuses*

544 Two distinct chambers (context A and context B) positioned inside sound attenuating
545 boxes were used during the Optimal Conditioning experiments. Context A consisted of a
546 small operant chamber (34 cm high x 25 cm wide x 23 cm deep, 200 lux, Med
547 Associates, see schematic drawing in Fig. 2A top) with one of the two aluminum walls
548 covered by black adhesive paper and two transparent acrylic walls, and a metal grid
549 floor beneath which a microcentrifuge tube (Eppendorf) containing 50 µl of 10% amyl
550 acetate (Sigma-Aldrich) was positioned. Context B consisted of a larger acrylic operant
551 chamber (40 cm high x 50 cm wide x 26 cm deep, 20 lux, Med Associates, see
552 schematic drawing in Fig. 2A bottom) with one of its walls covered by a black and white
553 stripped paper, and a floor made of a white acrylic board beneath which a
554 microcentrifuge tube (Eppendorf) containing 50 µl of deionized water was positioned.

555

556 *Procedures*

557 On day 0, rats were placed in context A for a 20-min familiarization session. Next, rats
558 were assigned to three experimental groups by matching their baseline freezing and
559 locomotor activity during the familiarization session: Full Conditioning (FC), Partial
560 Conditioning (PC), and Optimal Partial Conditioning (OPC). On day 1, rats were placed
561 into context A and exposed to one nonreinforced habituation tone (3 kHz, 75 dB, 30 s)
562 followed by distinct fear conditioning protocols (44 min duration). The FC group received

563 eight presentations of a conditioned stimulus (CS, 3 kHz tone, 75 dB, 30 s) that co-
564 terminated with an unconditioned stimulus (US, footshock, 0.7 mA, 0.5 s), with fixed ITIs
565 of 270 s. The PC group received four similar CS-US pairings with the same ITIs of 270
566 s, and remained in the chamber until the end of the session. The OPC group received
567 four similar CS-US pairings with ITIs of 8, 8, and 16 min. On day 2, rats were placed in
568 context B and given two CS presentations (ITI of 150 s, 7 min duration) in the absence
569 of US to test the retrieval of tone-associated fear memory in a novel context. On day 3,
570 rats were returned to context A for an extinction training session where they received
571 twelve CS presentations (ITIs of 150 s, 37 min duration). The first four CSs were
572 compared to the last four CSs to assess extinction learning within the same session. On
573 day 4 and 5, rats were placed back in context A and B, respectively, and exposed to an
574 extinction retrieval session (similar to day 2). On day 29 and 30, rats were placed back
575 in context A and B, respectively, and exposed to a spontaneous recovery session
576 (similar to day 2). On day 1 and day 2, rats in the same group were trained
577 simultaneously in four chambers with the group order counterbalanced to avoid
578 interference from different protocols in neighboring chambers. On the following days,
579 rats were simultaneously tested in four chambers regardless of the group assignment.
580 Each rat was tested in the exact same chamber across the days. Footshocks, tones,
581 intertrial intervals, and session duration were controlled by an automated video tracking
582 system (ANY-maze, Stoelting), which also quantified the percentage of time freezing,
583 distance traveled, average speed and maximum speed. All rats passed the criteria of
584 20% of freezing during at least one CS of the fear conditioning session and the first two
585 CSs of the extinction session.

586

587 ***Optimal vs. Spaced Partial Conditioning***

588 *Apparatus and Procedures*

589 The same apparatus and contexts described above were used. Following familiarization
590 on Day 0, rats were randomly assigned to two groups: Optimal Partial Conditioning
591 (OPC) and Spaced Partial Conditioning (SPC). The same procedures described above
592 were used here, except that: *i)* the footshock intensity was reduced from 0.7 mA to 0.5
593 mA to decrease the possibility of ceiling effects; *ii)* the SPC group received four CS-US
594 pairings with ITIs of 11 min and 10 s. The same automated video tracking system (ANY-
595 maze, Stoelting) described above was used for protocol control and behavioral
596 quantification. One rat that failed the criteria of 20% of freezing during at least one CS of
597 the fear conditioning session and the first two CSs of the extinction session was
598 excluded from the analyses.

599

600 ***Optimal Extinction***

601 *Lever-press training*

602 Rats were placed in an acrylic/aluminum operant chamber (34 cm high x 25 cm wide x
603 23 cm deep, Med Associates, see schematic drawing in Fig. 4A) and trained to press a
604 lever for sucrose on a fixed ratio of one pellet for each press. Next, animals were trained
605 in a variable interval schedule of reinforcement that was gradually reduced across the
606 days (one pellet every 15 s, 30 s, or 60 s) until they reached a minimum criterion of 10
607 presses/min after 7 days of training. All sessions lasted 30 min and were performed on

consecutive days. Sucrose pellet delivery, variable intervals, and session duration were controlled by an automated video tracking system (ANY-maze, Stoelting).

Apparatus and Procedure

On day 8, rats were placed into the same chamber where they had previously undergone lever presses training. Animals were exposed to five nonreinforced habituation tones (3 kHZ, 75 dB, 30 s duration) followed by seven CS-US pairings (ITIs of 150 s, 37 min duration). The footshock intensity was increased from 0.7 mA to 1.0-1.2 mA to result in stronger fear acquisition and consequently higher freezing levels during the extinction training session in the next day. Rats were assigned to three experimental groups by matching their freezing and lever presses during the fear conditioning session: Full Extinction (FE), Partial Extinction (PE), and Optimized Partial Extinction (OPE). On day 9, rats were returned to the same chamber for a fear extinction session (39 min duration). The FE group received twelve CSs with ITIs of 150 s; the PE group received four CSs with ITIs of 150 s and remained in the chamber until the end of the session; and the OPE group received four CSs with ITIs of 8, 8, and 16 min. On day 10 and 35, rats were placed into the same chamber and received two CSs with an ITI of 150 s to test the strength of fear extinction memory during extinction retrieval and spontaneous recovery tests, respectively. The same automated video tracking system (ANY-maze, Stoelting) described above was used for protocol control and behavioral quantification. Two rats that never reached the criterium of 20% of freezing during at least one CS of the fear conditioning session and the first two CSs of the extinction session were excluded from the analyses.

Quantification and statistical analysis

Rats were recorded with digital video cameras (Logitech C920) and behavioral indices were measured using automated video-tracking system (ANY-maze). Lever presses per minute were calculated by measuring the number of presses during the 30 s cue (or 30 s pre-cue) multiplied by two. All graphics and numerical values reported in the figures are presented as mean ± standard error of the mean (SEM). Grubbs' tests were used to identify outliers ($p < 0.05$) in each experiment and one rat in Fig. 2 was removed after identified by the test. Shapiro-Wilk test were performed to determine whether the data have a normal distribution. F tests before pair-wise comparison and Brown-Forsythe tests before multiple group comparison were performed to test if groups have the same variance. Statistical significance for parametric distributions was determined with paired Student's t test, Welch's t test, one-way analysis of variance (ANOVA) or two-way repeated-measures ANOVA followed by Tukey post-hoc comparisons, whereas Kruskal-Wallis test followed by Dunn's post-hoc test was used for non-parametric distributions (Prism 7), as indicated for each experiment. Sample size was based on estimations from previous literature and experience.

Data availability

All data that support the findings presented in this study are available from the corresponding author on reasonable request. Source codes will be submitted to the ModelDB database (85), and to GitHub (https://github.com/Owenxz/Zhang-XO-Enhanced-Learning-2022.git).

ACKNOWLEDGEMENT

We thank Nikita Watson and Sharon Gordon for their technical and administrative assistance. We also thank current members of the Byrne and Do Monte and Labs for their valuable comments on the manuscript. This work was supported by NIH grant R01-NS102490 to J.H.B, and NIH grant R00-MH105549, NIH grant R01-MH120136, a Brain & Behavior Research Foundation grant (NARSAD Young Investigator), and a Rising STARs Award from UT System to F.H.D-M.

REFERENCES

1. S. J. Martin, P. D. Grimwood, R. G. Morris, Synaptic plasticity and memory: an evaluation of the hypothesis. *Annu Rev Neurosci* **23**, 649-711 (2000).
2. E. R. Kandel, The molecular biology of memory storage: a dialogue between genes and synapses. *Science* **294**, 1030-1038 (2001).
3. M. A. Lynch, Long-term potentiation and memory. *Physiol Rev* **84**, 87-136 (2004).
4. C. M. Alberini, Transcription factors in long-term memory and synaptic plasticity. *Physiol Rev* **89**, 121-145 (2009).
5. J. H. Byrne, R. D. Hawkins, Nonassociative learning in invertebrates. *Cold Spring Harb Perspect Biol* **7** (2015).
6. S. Sharif, A. Guirguis, S. Fergus, F. Schifano, The use and impact of cognitive enhancers among university students: a systematic review. *Brain Sci* **11** (2021).
7. J. C. Lauterborn *et al.*, Chronic ampakine treatments stimulate dendritic growth and promote learning in middle-aged rats. *J Neurosci* **36**, 1636-1646 (2016).
8. J. L. McGaugh, L. F. Petrinovich, Effects of drugs on learning and memory. *Int Rev Neurobiol* **8**, 139-196 (1965).
9. G. Lynch, C. D. Cox, C. M. Gall, Pharmacological enhancement of memory or cognition in normal subjects. *Front Syst Neurosci* **8**, 90 (2014).
10. S. M. Fernandez *et al.*, Estradiol-induced enhancement of object memory consolidation involves hippocampal extracellular signal-regulated kinase activation and membrane-bound estrogen receptors. *J Neurosci* **28**, 8660-8667 (2008).

11. M. T. Brown *et al.*, Ventral tegmental area GABA projections pause accumbal cholinergic interneurons to enhance associative learning. *Nature* **492**, 452-456 (2012).

12. S. Nabavi *et al.*, Engineering a memory with LTD and LTP. *Nature* **511**, 348-352 (2014).

13. K. Lee *et al.*, Parvalbumin interneurons modulate striatal output and enhance performance during associative learning. *Neuron* **93**, 1451-1463 e1454 (2017).

14. X. Liu *et al.*, Optogenetic stimulation of a hippocampal engram activates fear memory recall. *Nature* **484**, 381-385 (2012).

15. P. Smolen, Y. Zhang, J. H. Byrne, The right time to learn: mechanisms and optimization of spaced learning. *Nat Rev Neurosci* **17**, 77-88 (2016).

16. P. Smolen, D. A. Baxter, J. H. Byrne, Comparing theories for the maintenance of late LTP and long-term memory: computational analysis of the roles of kinase feedback pathways and synaptic reactivation. *Front Comput Neurosci* **14**, 569349 (2020).

17. Y. Zhang, P. D. Smolen, L. J. Cleary, J. H. Byrne, Quantitative description of the interactions among kinase cascades underlying long-term plasticity of *Aplysia* sensory neurons. *Sci Rep* **11**, 14931 (2021).

18. S. Schacher, V. F. Castellucci, E. R. Kandel, cAMP evokes long-term facilitation in *Aplysia* sensory neurons that requires new protein synthesis. *Science* **240**, 1667-1669 (1988).

708 19. B. A. Goldsmith, T. W. Abrams, Reversal of synaptic depression by serotonin at
709 Aplysia sensory neuron synapses involves activation of adenylyl cyclase. *Proc*
710 *Natl Acad Sci U S A* **88**, 9021-9025 (1991).
711 20. U. Muller, T. J. Carew, Serotonin induces temporally and mechanistically distinct
712 phases of persistent PKA activity in *Aplysia* sensory neurons. *Neuron* **21**, 1423-
713 1434 (1998).
714 21. K. C. Martin *et al.*, MAP kinase translocates into the nucleus of the presynaptic
715 cell and is required for long-term facilitation in *Aplysia*. *Neuron* **18**, 899-912
716 (1997).
717 22. S. K. Sharma, T. J. Carew, The roles of MAPK cascades in synaptic plasticity
718 and memory in *Aplysia*: facilitatory effects and inhibitory constraints. *Learn Mem*
719 **11**, 373-378 (2004).
720 23. S. K. Sharma *et al.*, Differential role of mitogen-activated protein kinase in three
721 distinct phases of memory for sensitization in *Aplysia*. *J Neurosci* **23**, 3899-3907
722 (2003).
723 24. P. K. Dash, B. Hochner, E. R. Kandel, Injection of the cAMP-responsive element
724 into the nucleus of *Aplysia* sensory neurons blocks long-term facilitation. *Nature*
725 **345**, 718-721 (1990).
726 25. D. Bartsch *et al.*, Aplysia CREB2 represses long-term facilitation: relief of
727 repression converts transient facilitation into long-term functional and structural
728 change. *Cell* **83**, 979-992 (1995).

729 26. R. Y. Liu, L. J. Cleary, J. H. Byrne, The requirement for enhanced CREB1
730 expression in consolidation of long-term synaptic facilitation and long-term
731 excitability in sensory neurons of *Aplysia*. *J Neurosci* **31**, 6871-6879 (2011).
732 27. G. T. Philips, E. I. Tzvetkova, T. J. Carew, Transient mitogen-activated protein
733 kinase activation is confined to a narrow temporal window required for the
734 induction of two-trial long-term memory in *Aplysia*. *J Neurosci* **27**, 13701-13705
735 (2007).
736 28. Y. Zhang *et al.*, Computational design of enhanced learning protocols. *Nat*
737 *Neurosci* **15**, 294-297 (2011).
738 29. G. E. Schafe, J. E. LeDoux, Memory consolidation of auditory pavlovian fear
739 conditioning requires protein synthesis and protein kinase A in the amygdala. *J*
740 *Neurosci* **20**, RC96 (2000).
741 30. T. Abel *et al.*, Genetic demonstration of a role for PKA in the late phase of LTP
742 and in hippocampus-based long-term memory. *Cell* **88**, 615-626 (1997).
743 31. J. P. Adams, J. D. Sweatt, Molecular psychology: roles for the ERK MAP kinase
744 cascade in memory. *Annu Rev Pharmacol Toxicol* **42**, 135-163 (2002).
745 32. S. Impey *et al.*, Cross talk between ERK and PKA is required for Ca^{2+} stimulation
746 of CREB-dependent transcription and ERK nuclear translocation. *Neuron* **21**,
747 869-883 (1998).
748 33. E. D. Roberson, J. D. Sweatt, Transient activation of cyclic AMP-dependent
749 protein kinase during hippocampal long-term potentiation. *J Biol Chem* **271**,
750 30436-30441 (1996).

751 34. S. I. Vázquez, A. Vázquez, S. Peña de Ortiz, Different hippocampal activity
752 profiles for PKA and PKC in spatial discrimination learning. *Behavioral*
753 *Neuroscience* **114**, 1109-1118 (2000).
754 35. Y. Wang *et al.*, A molecular brake controls the magnitude of long-term
755 potentiation. *Nat Commun* **5**, 3051 (2014).
756 36. B. Milner, L. R. Squire, E. R. Kandel, Cognitive neuroscience and the study of
757 memory. *Neuron* **20**, 445-468 (1998).
758 37. A. Mayes, D. Montaldi, E. Migo, Associative memory and the medial temporal
759 lobes. *Trends Cogn Sci* **11**, 126-135 (2007).
760 38. K. Nakazawa *et al.*, Requirement for hippocampal CA3 NMDA receptors in
761 associative memory recall. *Science* **297**, 211-218 (2002).
762 39. S. M. Ajay, U. S. Bhalla, A role for ERKII in synaptic pattern selectivity on the
763 time-scale of minutes. *Eur J Neurosci* **20**, 2671-2680 (2004).
764 40. J. A. Detert, N. D. Kampa, J. R. Moyer, Jr., Differential effects of training intertrial
765 interval on acquisition of trace and long-delay fear conditioning in rats. *Behav*
766 *Neurosci* **122**, 1318-1327 (2008).
767 41. T. B. Lonsdorf *et al.*, Don't fear 'fear conditioning': Methodological considerations
768 for the design and analysis of studies on human fear acquisition, extinction, and
769 return of fear. *Neurosci Biobehav Rev* **77**, 247-285 (2017).
770 42. R. G. Phillips, J. E. LeDoux, Differential contribution of amygdala and
771 hippocampus to cued and contextual fear conditioning. *Behav Neurosci* **106**,
772 274-285 (1992).

43. N. R. Selden, B. J. Everitt, L. E. Jarrard, T. W. Robbins, Complementary roles for the amygdala and hippocampus in aversive conditioning to explicit and contextual cues. *Neuroscience* **42**, 335-350 (1991).

44. S. Maren, K. L. Phan, I. Liberzon, The contextual brain: implications for fear conditioning, extinction and psychopathology. *Nat Rev Neurosci* **14**, 417-428 (2013).

45. N. J. Cepeda, H. Pashler, E. Vul, J. T. Wixted, D. Rohrer, Distributed practice in verbal recall tasks: A review and quantitative synthesis. *Psychol Bull* **132**, 354-380 (2006).

46. M. Raman *et al.*, Teaching in small portions dispersed over time enhances long-term knowledge retention. *Med Teach* **32**, 250-255 (2010).

47. M. J. Anderson, S. A. Jablonski, D. B. Klimas, Spaced initial stimulus familiarization enhances novelty preference in Long-Evans rats. *Behav Processes* **78**, 481-486 (2008).

48. L. Jiang *et al.*, Spaced training enhances contextual fear memory via activating hippocampal 5-HT2A receptors. *Front Mol Neurosci* **12**, 317 (2019).

49. M. T. Scharf *et al.*, Protein synthesis is required for the enhancement of long-term potentiation and long-term memory by spaced training. *J Neurophysiol* **87**, 2770-2777 (2002).

50. C. K. Cain, A. M. Blouin, M. Barad, Temporally massed CS presentations generate more fear extinction than spaced presentations. *J Exp Psychol Anim Behav Process* **29**, 323-333 (2003).

795 51. L. de Oliveira Alvares, F. H. Do-Monte, Understanding the dynamic and destiny
796 of memories. *Neurosci Biobehav Rev* **125**, 592-607 (2021).
797 52. G. J. Quirk, D. Mueller, Neural mechanisms of extinction learning and retrieval.
798 *Neuropsychopharmacology* **33**, 56-72 (2008).
799 53. D. E. Berman, Y. Dudai, Memory extinction, learning anew, and learning the new:
800 dissociations in the molecular machinery of learning in cortex. *Science* **291**,
801 2417-2419 (2001).
802 54. J. F. Flood, M. E. Jarvik, E. L. Bennett, A. E. Orme, M. R. Rosenzweig, Protein
803 synthesis inhibition and memory for pole jump active avoidance and extinction.
804 *Pharmacol Biochem Behav* **7**, 71-77 (1977).
805 55. J. Radulovic, N. C. Tronson, Molecular specificity of multiple hippocampal
806 processes governing fear extinction. *Rev Neurosci* **21**, 1-17 (2010).
807 56. E. Santini, R. U. Muller, G. J. Quirk, Consolidation of extinction learning involves
808 transfer from NMDA-independent to NMDA-dependent memory. *J Neurosci* **21**,
809 9009-9017 (2001).
810 57. G. Szapiro, M. R. Vianna, J. L. McGaugh, J. H. Medina, I. Izquierdo, The role of
811 NMDA glutamate receptors, PKA, MAPK, and CAMKII in the hippocampus in
812 extinction of conditioned fear. *Hippocampus* **13**, 53-58 (2003).
813 58. N. C. Tronson *et al.*, Regulatory mechanisms of fear extinction and depression-
814 like behavior. *Neuropsychopharmacology* **33**, 1570-1583 (2008).
815 59. E. Santini, H. Ge, K. Ren, S. Pena de Ortiz, G. J. Quirk, Consolidation of fear
816 extinction requires protein synthesis in the medial prefrontal cortex. *J Neurosci*
817 **24**, 5704-5710 (2004).

818 60. A. Holmes, G. J. Quirk, Pharmacological facilitation of fear extinction and the
819 search for adjunct treatments for anxiety disorders--the case of yohimbine.
820 *Trends Pharmacol Sci* **31**, 2-7 (2010).
821 61. F. H. Do-Monte, G. Manzano-Nieves, K. Quinones-Laracuente, L. Ramos-
822 Medina, G. J. Quirk, Revisiting the role of infralimbic cortex in fear extinction with
823 optogenetics. *J Neurosci* **35**, 3607-3615 (2015).
824 62. M. Mast, R. J. Blanchard, D. C. Blanchard, The relationship of freezing and
825 response suppression in a CER situation. *The Psychological Record* **32**, 151
826 (1982).
827 63. F. Sotres-Bayon, D. Sierra-Mercado, E. Pardilla-Delgado, G. J. Quirk, Gating of
828 fear in prelimbic cortex by hippocampal and amygdala inputs. *Neuron* **76**, 804-
829 812 (2012).
830 64. G. J. Quirk, G. K. Russo, J. L. Barron, K. Lebron, The role of ventromedial
831 prefrontal cortex in the recovery of extinguished fear. *J Neurosci* **20**, 6225-6231
832 (2000).
833 65. C. A. Podlesnik, M. E. Kelley, C. Jimenez-Gomez, M. E. Bouton, Renewed
834 behavior produced by context change and its implications for treatment
835 maintenance: A review. *J Appl Behav Anal* **50**, 675-697 (2017).
836 66. T. D. Goode, S. Maren, Animal models of fear relapse. *ILAR J* **55**, 246-258
837 (2014).
838 67. M. A. Morgan, J. E. LeDoux, Differential contribution of dorsal and ventral medial
839 prefrontal cortex to the acquisition and extinction of conditioned fear in rats.
840 *Behav Neurosci* **109**, 681-688 (1995).

841 68. T. J. Carew, C. L. Sahley, Invertebrate learning and memory: from behavior to
842 molecules. *Annu Rev Neurosci* **9**, 435-487 (1986).
843 69. R. D. Hawkins, J. H. Byrne, Associative learning in invertebrates. *Cold Spring*
844 *Harb Perspect Biol* **7** (2015).
845 70. P. P. Verkoeijen, R. M. Rikers, H. G. Schmidt, Limitations to the spacing effect:
846 demonstration of an inverted u-shaped relationship between interrepetition
847 spacing and free recall. *Exp Psychol* **52**, 257-263 (2005).
848 71. P. B. Barela, Theoretical mechanisms underlying the trial-spacing effect in
849 Pavlovian fear conditioning. *J Exp Psychol Anim Behav Process* **25**, 177 (1999).
850 72. S. M. Ajay, U. S. Bhalla, A propagating ERKII switch forms zones of elevated
851 dendritic activation correlated with plasticity. *HFSP J* **1**, 49-66 (2007).
852 73. D. Genoux *et al.*, Protein phosphatase 1 is a molecular constraint on learning
853 and memory. *Nature* **418**, 970-975 (2002).
854 74. M. Davis, D. I. Astrachan, Conditioned fear and startle magnitude: effects of
855 different footshock or backshock intensities used in training. *J Exp Psychol Anim*
856 *Behav Process* **4**, 95-103 (1978).
857 75. S. Maren, Synaptic mechanisms of associative memory in the amygdala. *Neuron*
858 **47**, 783-786 (2005).
859 76. J. P. Johansen, C. K. Cain, L. E. Ostroff, J. E. LeDoux, Molecular mechanisms of
860 fear learning and memory. *Cell* **147**, 509-524 (2011).
861 77. N. Padilla-Coreano, F. H. Do-Monte, G. J. Quirk, A time-dependent role of
862 midline thalamic nuclei in the retrieval of fear memory. *Neuropharmacology* **62**,
863 457-463 (2012).

78. A. M. Woods, M. E. Bouton, Immediate extinction causes a less durable loss of performance than delayed extinction following either fear or appetitive conditioning. *Learn Mem* **15**, 909-920 (2008).

79. M. E. Bouton, S. Maren, G. P. McNally, Behavioral and neurobiological mechanisms of Pavlovian and instrumental extinction learning. *Physiol Rev* **101**, 611-681 (2021).

80. G. E. Schafe *et al.*, Activation of ERK/MAP kinase in the amygdala is required for memory consolidation of pavlovian fear conditioning. *J Neurosci* **20**, 8177-8187 (2000).

81. B. Di Benedetto *et al.*, Activation of ERK/MAPK in the lateral amygdala of the mouse is required for acquisition of a fear-potentiated startle response. *Neuropsychopharmacology* **34**, 356-366 (2009).

82. R. C. Malenka *et al.*, An essential role for postsynaptic calmodulin and protein kinase activity in long-term potentiation. *Nature* **340**, 554-557 (1989).

83. S. Wang, T. Sheng, S. Ren, T. Tian, W. Lu, Distinct roles of PKCı/λ and PKMζ in the initiation and maintenance of hippocampal long-term potentiation and memory. *Cell Rep* **16**, 1954-1961 (2016).

84. B. Ermentrout, *Simulating, analyzing, and animating dynamical systems : a guide to XPPAUT for researchers and students*, Software, environments, tools (Society for Industrial and Applied Mathematics, Philadelphia, 2002), pp. xiv, 290 p.

85. R. A. McDougal, T. M. Morse, M. L. Hines, G. M. Shepherd, ModelView for ModelDB: online presentation of model structure. *Neuroinformatics* **13**, 459-470 (2015).

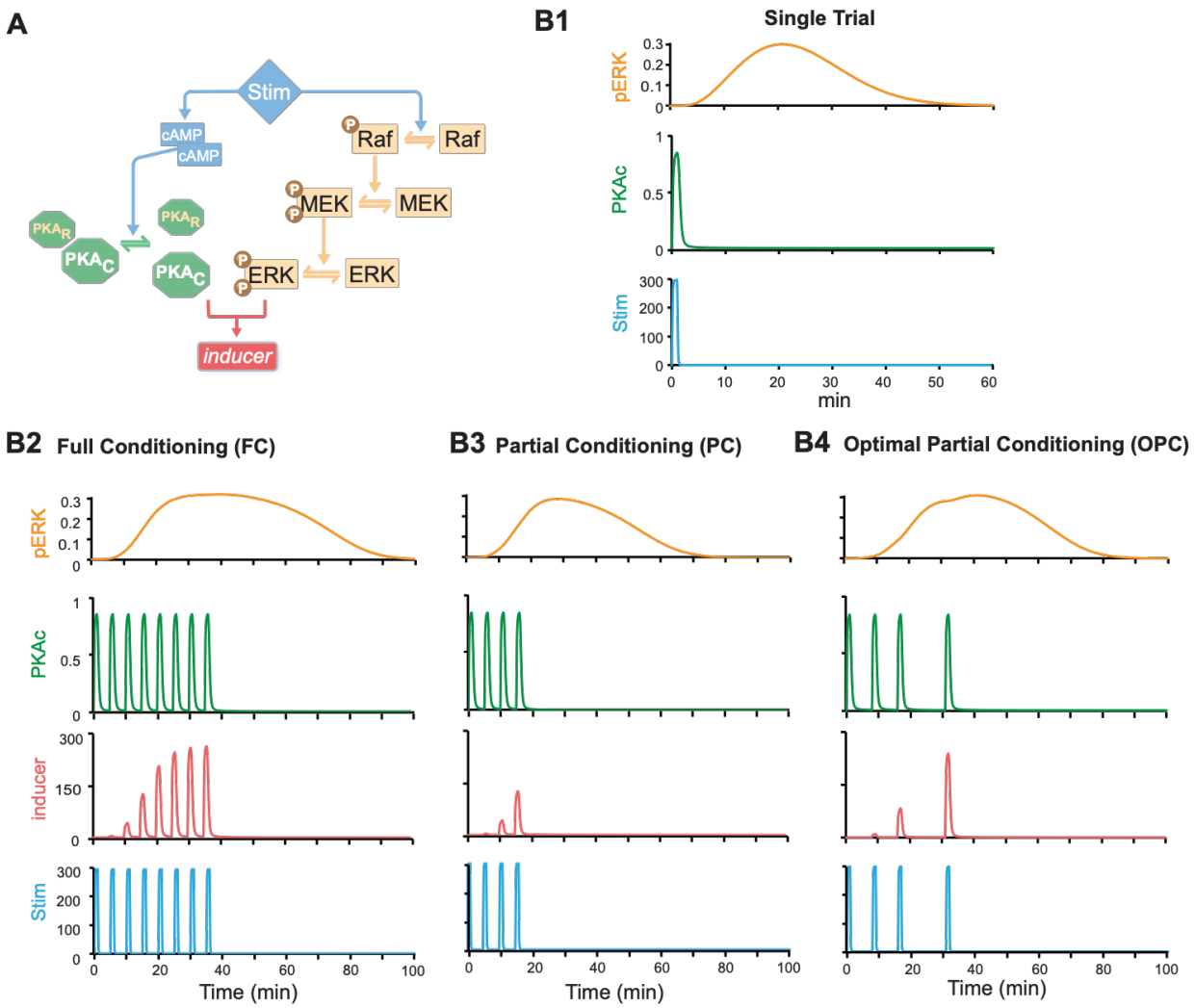

887

888 **Figure 1. Computational simulations of PKA and ERK pathways predict an optimal protocol for**
889 **fear conditioning. A**, Schematic of the model. Stimulus (*Stim*) activates PKA via cAMP and activates
890 ERK via Raf-MEK. The variable *inducer* quantifies the PKA/ERK interaction (activity overlap). **B1**,
891 Simulated time courses of activated ERK (pERK, orange traces, μM) and activated PKA (PKAc, green
892 traces) in response to one trial of *Stim* (μM). **B2**, Simulated time courses of pERK (orange traces, μM),
893 PKAc (green traces) and *inducer* (red traces, nM) in response to an 8-trial protocol with regular ITIs of 4.5
894 min (full conditioning, FC). **B3**, Simulated time courses of pERK (orange traces), PKAc (green traces),
895 and *inducer* (red traces) in response to a 4-trial protocol with regular ITIs of 4.5 min (partial conditioning,
896 PC). **B4**, Simulated time courses of pERK (orange traces), PKAc (green traces) and *inducer* (red traces)

in response to a 4-trial protocol with computationally designed intervals (optimal partial conditioning, OPC).

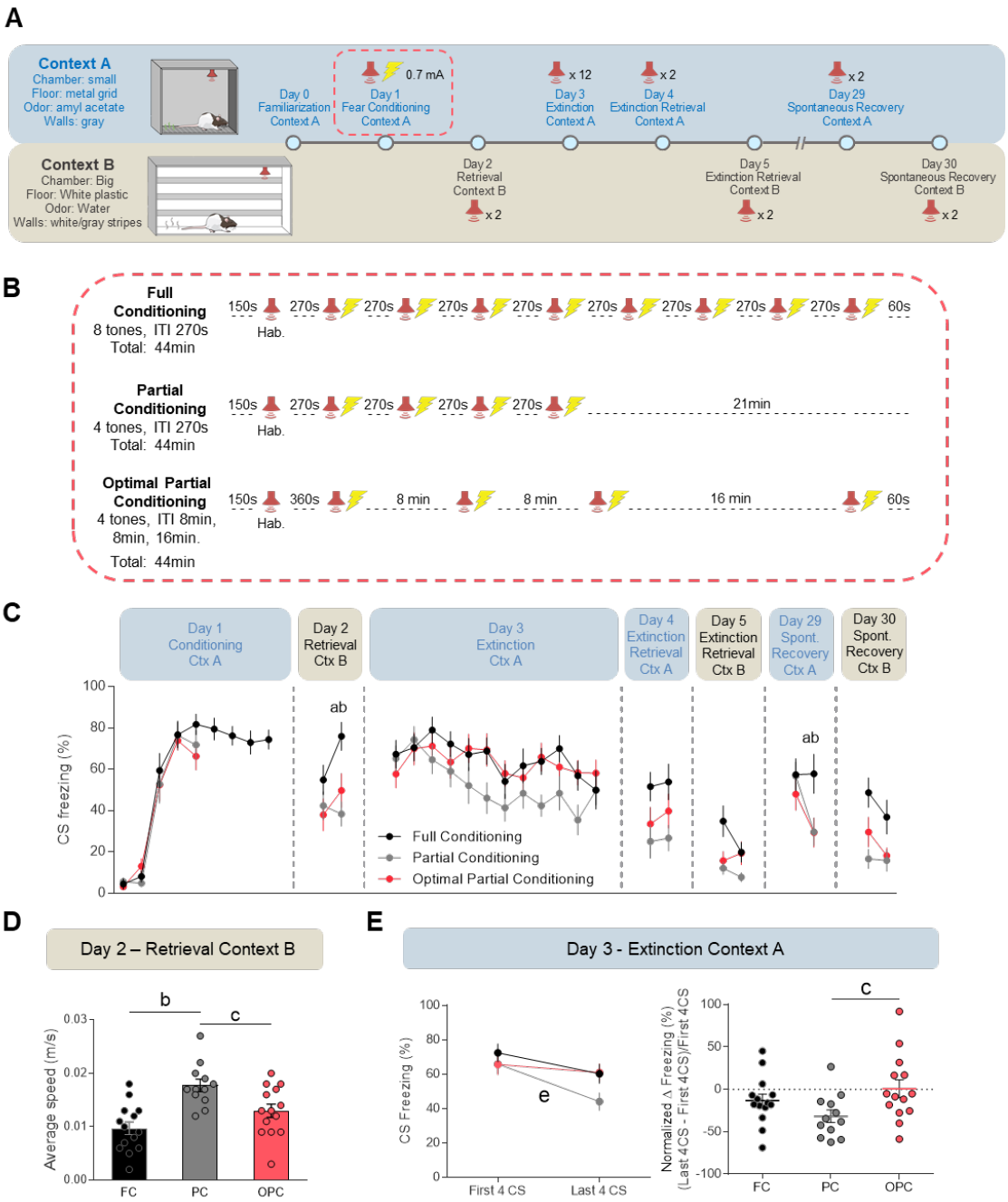

Figure 2. Computationally designed protocol enhanced fear conditioning in rats. **A,** Schematics of the enhanced fear conditioning experimental procedures. Top: tests that were conducted in Context A. Bottom: tests that were conducted in Context B. **B,** Schematics of the fear conditioning protocols for full conditioning (FC, n = 14), partial conditioning (PC, n = 12), and optimal partial conditioning groups (OPC, n = 14). Following a habituation (Hab.) tone, rats received multiple trials of a conditioned stimulus (CS, 3 kHz tone, 30 s) that co-terminated with an unconditioned stimulus (US, footshock, 0.7 mA, 0.5 s). **C,**

927 Freezing levels during CS presentations of each group across the experiment. Two-way Repeated-
928 Measure ANOVA for each day followed by Tukey's post hoc test. Letters a, b, and c indicate pairwise
929 post hoc tests with $p < 0.05$: a, FC vs. OPC; b, FC vs. PC; c, OPC vs. PC. **D,** OPC group shows lower
930 average speed compared to PC group. One-way ANOVA followed by Tukey post hoc test. Letters b and c
931 indicate pairwise tests with $p < 0.05$: b, FC vs. PC ; c, OPC vs. PC. **E,** OPC group is resistant to extinction
932 while PC group shows significantly more extinction. Left, the freezing levels during the first 4 and last 4
933 CS presentations. Paired Student's t test. Letter e indicates test with $p < 0.05$: PC, Last 4 CS vs. First 4
934 CS. Right, normalized change of the freezing level during extinction, as indicated by the difference of the
935 freezing levels between last 4 and first 4 CS presentations as a percentage of the freezing level of the
936 first 4 CS presentations. One-way ANOVA followed by Tukey's post hoc test. * $p<0.05$. Letter c indicates
937 pairwise test with $p < 0.05$: OPC vs. PC. Data shown here and in subsequent illustrations as mean ±
938 SEM.
939
940
941
942
943
944
945
946
947
948
949
950
951

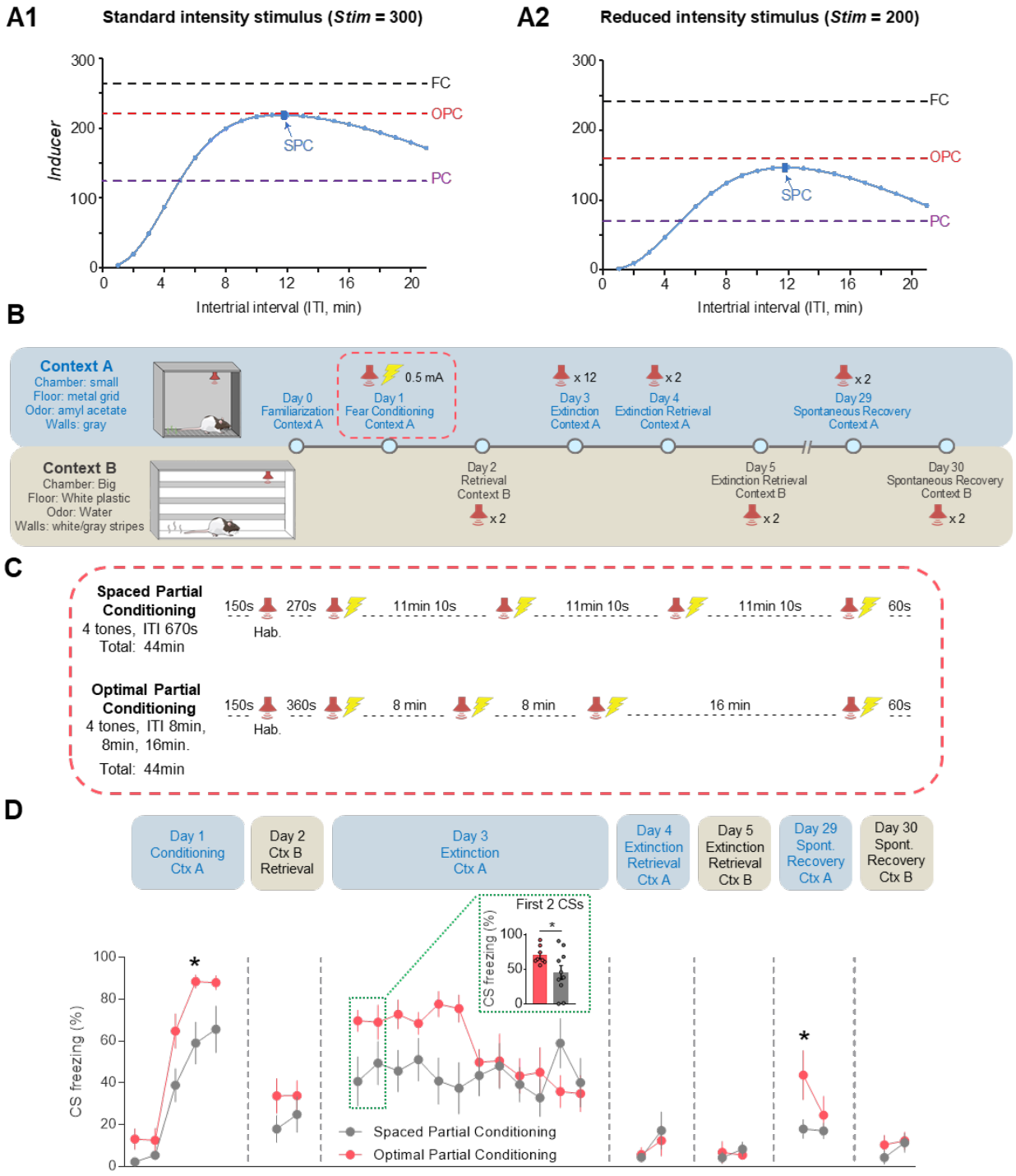

Figure 3. **Optimal partial conditioning protocol induced stronger fear memory than spaced partial conditioning protocol in rats**. **A**, *Inducer* peak levels from the FC, PC, and OPC protocols, compared to peak levels from partial conditioning protocols of 4 trials with regular ITIs varying from 1 to 21 min, using standard intensity stimulus (**A1**) or reduced intensity stimulus (**A2**). The peak *inducer* values of FC, PC,

957 and OPC are labeled by dashed lines (black: FC; red: OPC; purple: PC). The blue curve gives peak
958 *inducer* values for the protocols with regular ITIs, and the curve peaks at the dark blue dot and arrow,
959 representing the SPC protocol with equal ITIs of 11 min and 10 s. **B,** Schematics of the fear conditioning
960 procedures. Top: tests that were conducted in Context A. Bottom: tests that were conducted in Context B.
961 **C,** Schematics of the fear conditioning protocols for optimal partial conditioning (OPC, n = 8), and spaced
962 partial conditioning groups (SPC, n = 10, ITI = 670 s). Following a habituation (Hab.) tone, rats received 4
963 trials of a conditioned stimulus (CS, 3 kHz tone, 30 s) that co-terminated with an unconditioned stimulus
964 (US, footshock, 0.5 mA, 0.5 s). **D,** Freezing levels during CS presentations of each group across the
965 experiment; Two-way repeated-measure ANOVA for each day followed by Tukey's pairwise post hoc test,
966 * $p<0.05$. Inset: the average freezing level during the first two CS presentations; Welch's t test, * $p<0.05$.
967
968
969
970
971
972
973
974
975
976
977
978
979
980
981

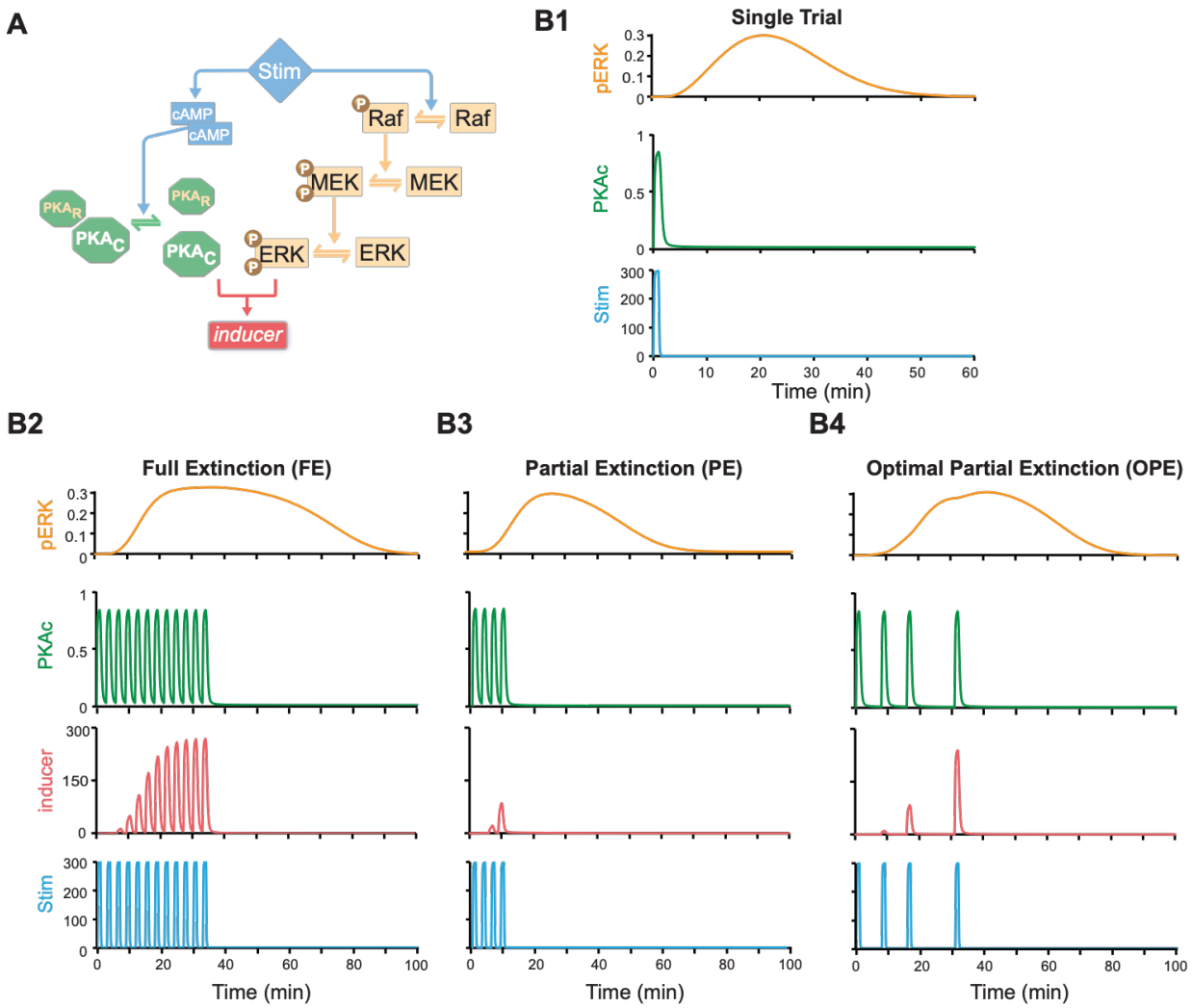

Figure 4. Prediction of enhanced protocol for fear extinction. A, Schematic of the model. **B1**, Simulated time courses of activated ERK (pERK, orange traces, μM) and activated PKA (PKAc, green traces) in response to one trial of *Stim* (μM). **B2**, Simulated time courses of pERK (orange traces, μM), PKAc (green traces) and *inducer* (red traces, nM) in response to 12-trial protocol with regular intervals of 2.5 min (full extinction, FE). **B3**, Simulated time courses of pERK (orange traces), PKAc (green traces) and *inducer* (red traces) in response to 4-trial protocol with regular intervals of 2.5 min (partial extinction, PE). **B4**, Simulated time courses of pERK (orange traces), PKAc (green traces) and *inducer* (red traces) in response to 4-trial protocol with computationally designed intervals (optimal partial extinction, OPE).

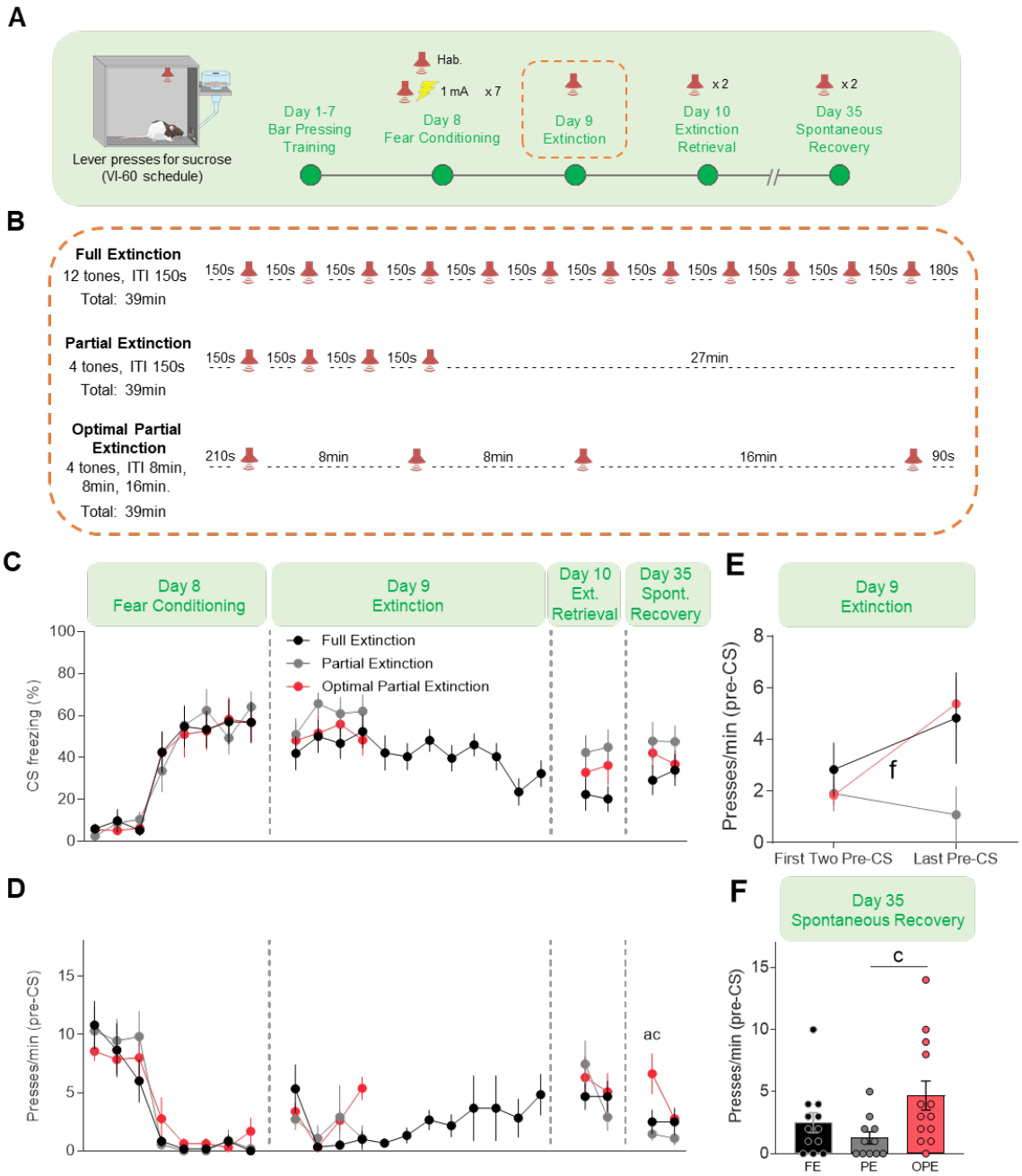

Figure 5. Computationally designed protocol enhanced fear extinction in rats. **A.** Schematic of the enhanced fear extinction experimental procedures. Rats were trained to constantly press a lever to retrieve sucrose pellets in a variable interval 60 (VI60) schedule, where the average interval between each sucrose delivery is 60 s. **B,** Schematics of the fear extinction protocols for full extinction (FE, n = 12), partial extinction (PE, n = 11), and optimal partial extinction groups (OPE, n = 13), during which rats received multiple trials of a conditioned stimulus (CS, 3 kHz tone, 30 s). **C,** Freezing levels during CS presentations of each group across the experiment. No significant difference between groups was found

by Two-way RM ANOVA. **D,** Lever presses rates during the 30s of each CS presentation (pre-CS period) of each group across the experiment. Two-way repeated-measure ANOVA for each day followed by Tukey's pairwise post hoc test. Letters a and c indicate pairwise tests with $p < 0.05$: a, FE vs. OPE ; c, OPE vs. PE. **E,** OPE group shows significant increase of pre-CS lever presses comparing the last CS presentation to the average lever press rate of the first two CS presentations. Paired Student's t test. Letter f indicates test with $p < 0.05$: OPC, Last 4 CS vs. First 4 CS. **F,** OPE group shows higher lever presses during pre-CS period compared to PE group in spontaneous recovery test. One-way ANOVA followed by Tukey's post hoc test. Letter c indicates pairwise comparison with * $p<0.05$: OPE vs. PE.

1024 **SUPPLEMENTARY FIGURES**

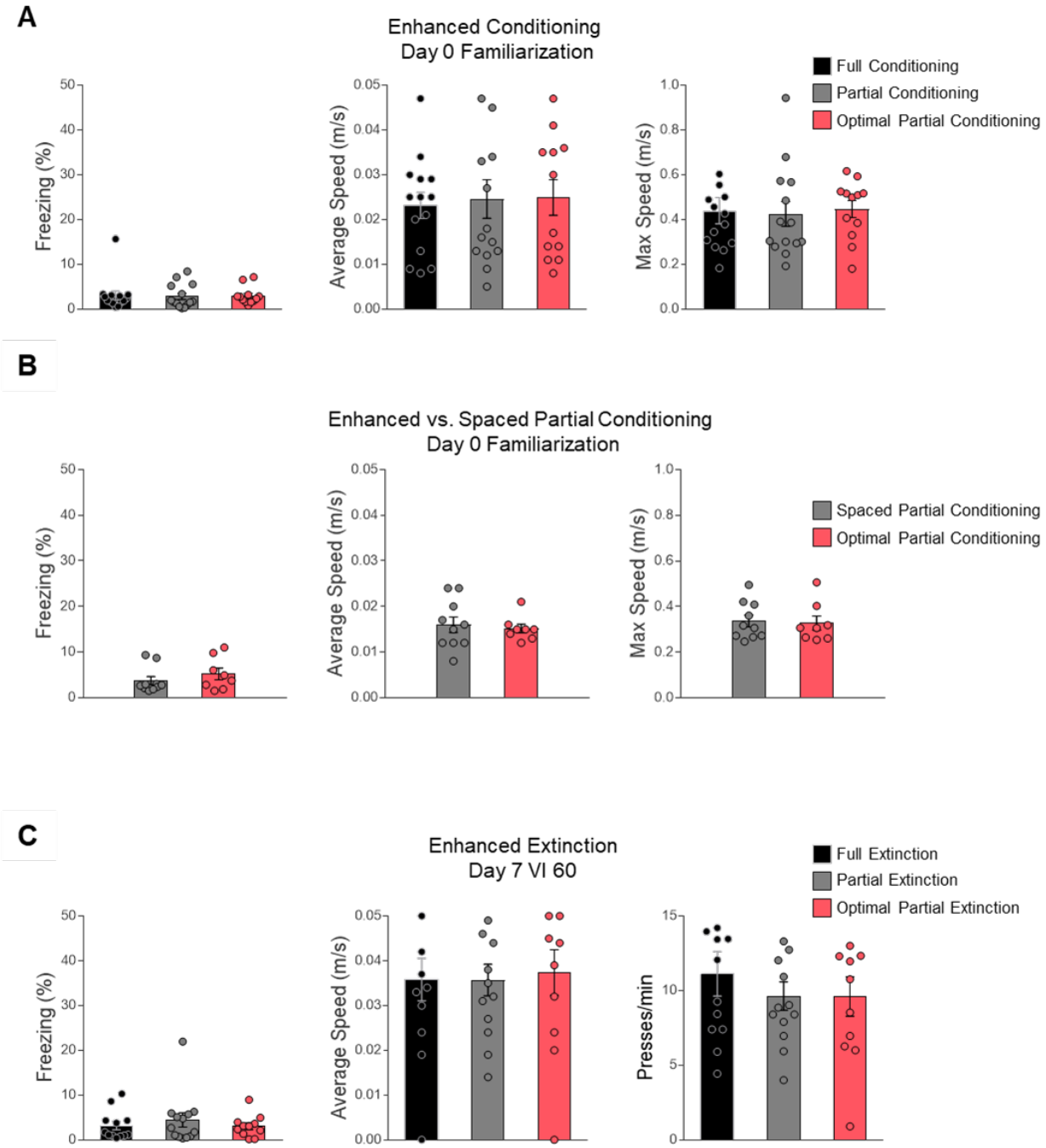

1025

1026 **Supplementary Figure 1. No difference of baseline activity between groups. A,** No differences in
1027 total freezing level (left), average speed (middle), and maximum speed (right) between the three groups
1028 were observed during familiarization of the enhanced conditioning experiment. **B,** No differences in total
1029 freezing level (left), average speed (middle), and maximum speed (right) were seen between the three

1030 groups during familiarization of the enhanced vs. spaced conditioning experiment. **C,** No differences in
1031 total freezing level (left), average speed (middle), and rate of lever presses (right) were observed between
1032 the three groups during the last day of lever presses training of the enhanced extinction experiment. One-
1033 way ANOVA. Data shown as mean ± SEM.
1034
1035
1036
1037
1038
1039
1040
1041
1042
1043
1044
1045
1046
1047
1048
1049
1050
1051

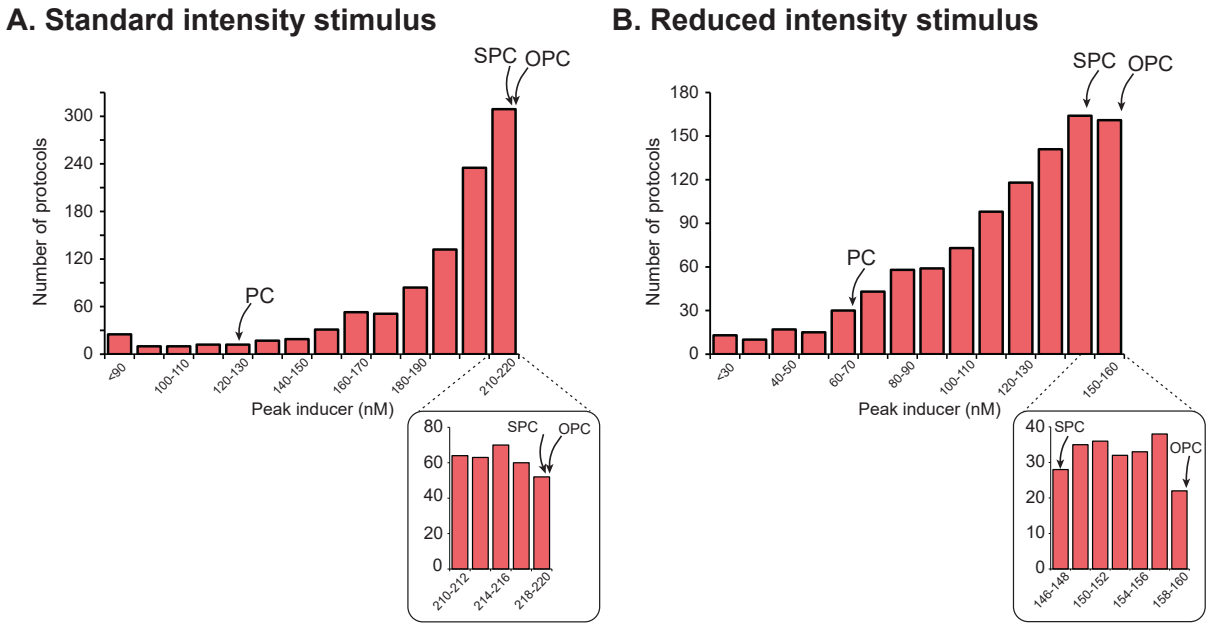

Supplementary Figure 2. **Histogram of peak levels of *inducer* from 1,000 protocols. A**, Standard intensity stimulus (*Stim* = 300 μM). The range of peak levels of *inducer* (0 - 220 nM) was subdivided into 14 bins, and the number of simulations that produced a peak concentration of *inducer* in each subdivision was plotted. The arrows indicate which bins contained the peak concentrations produced by the partial conditioning, spaced partial conditioning (SPC), and the optimal partial conditioning (OPC) protocols. **B,** Reduced intensity stimulus (*Stim* = 200 μM). The range of peak levels of *inducer* (0 - 160 nM) was subdivided into 14 bins, and the number of simulations that produced a peak concentration of *inducer* in each subdivision was plotted. Insets below the main plots illustrate in detail the difference in peak *inducer* for SPC *vs*. OPC, which is negligible in **A**.

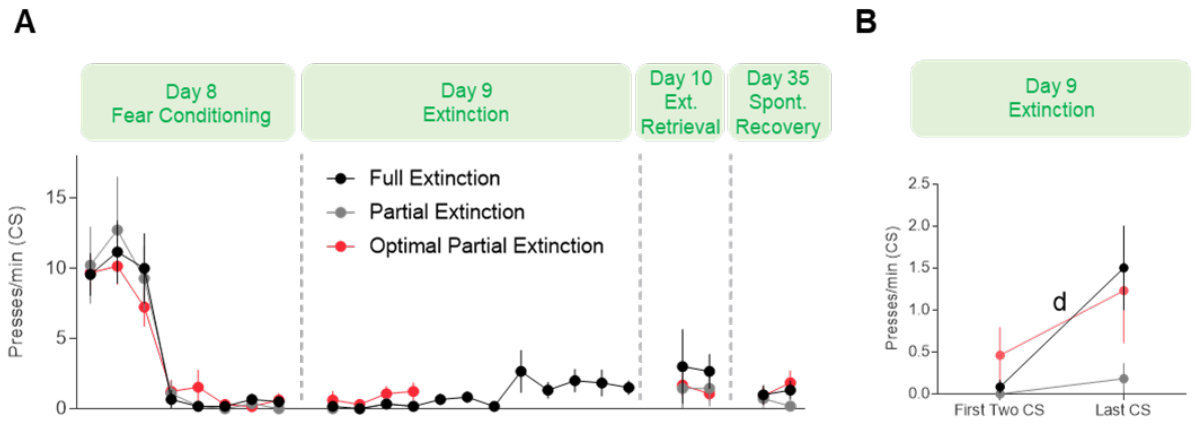

Supplementary Figure 3. Lever press during CS presentations in enhanced extinction experiment. **A**, Lever presses rates during CS presentations of each group across the experiment. Two-way repeated-measure ANOVA for each day found no difference among groups. **B,** FE group shows significant increase of CS lever presses comparing the last CS presentation to the average lever press rate of the first two CS presentations. Paired Student's t test. Letter d indicates test with $p < 0.05$: d, FE, Last 4 CS vs. first 4 CS.